Scientific Research Publishing

Open Journal of Geology, 2023, 13, 276-286
https://www.scirp.org/journal/ojg
ISSN Online: 2161-7589
ISSN Print: 2161-7570

Analysis of a Pull-Apart Basin and Its Associated Fractures in the Woodford Shale, Central Oklahoma

Rulang Wang[1,2], Feng Qin[3], Nianfa Yang[1*], Yun Zhou[1]

[1]State Key Laboratory of Petroleum Resources and Prospecting, College of Geosciences, China University of Petroleum, Beijing, China
[2]Zhejiang Mercantile Exchange, Zhoushan, China
[3]Exploration and Development Research Institute, Shengli Oilfield Company, SINOPEC, Dongying, China
Email: *nianfayang@student.cup.edu.cn

How to cite this paper: Wang, R.L., Qin, F., Yang, N.F. and Zhou, Y. (2023) Analysis of a Pull-Apart Basin and Its Associated Fractures in the Woodford Shale, Central Oklahoma. *Open Journal of Geology*, **13**, 276-286.
https://doi.org/10.4236/ojg.2023.134013

Received: March 20, 2023
Accepted: April 17, 2023
Published: April 20, 2023

Abstract

Pull-apart basins are faulting and folding zones with high intensity of fractures that strongly affect the production in unconventional shale gas. While most observations of pull-apart basins were from surface mapping or laboratory experiments, we investigated a nascent pull-apart basin in the subsurface. We characterized a nascent pull-apart basin along the strike-slip fault within the Woodford Shale by using seismic attributes analyses, including coherence, dip-azimuth, and curvature. The results indicate a 32 km long, N-S striking strike-slip fault that displays a distinct but young pull-apart basin, which is ~1.6 km by 3.2 km in size and is bounded by two quasi-circular faults. The curvature attribute map reveals two quasi-circular folds, which depart from the main strike-slip fault at ~25˚, resulting in an elliptical basin. Inside the basin, a series of echelon quasi-circular normal faults step into the bottom of the basin with ~80 m of total subsidence. We propose that the controls of the shape of pull-apart basin are the brittleness of the shale, and we suggest proper seismic attributes as a useful tool for investigating high fracture intensity in the subsurface for hydrofracturing and horizontal drilling within the shale.

Keywords

Pull-Apart Basin, Seismic Attributes, Analog Model, Fractures, Shale Gas

1. Introduction

The Woodford Shale in central Oklahoma exhibits complex faulted structure in

3D seismic attributes analysis. While the attributes are effective in mapping large scale discontinuities within shale reservoirs, they are ineffective in the detection of sub-seismic fractures, which could be critical for gas production. We complemented this limitation of seismic attributes analysis by using laboratory clay models, and present an integrated seismic-experimental study of a pull-apart basin that developed along a large strike-slip fault within the Woodford Shale [1] [2].

Pull-apart basin is a fundamental structure developed by connecting two major strike-slip faults. The geometry of the evolution is mostly studied by implementing wet-clay models or sandboxes [3] [4] [5] [6], which has been used in analog structure characteristics. Clay material is used for its consistency of low strength, and easy handling and preparation. [7] first explained the pull-apart basins mapped in California. [4] applied the models to explain pull-apart basins in Dead Sea. [6] used detailed model features to interpret the Imperial Valley of California, Hope Fault of New Zealand, and Vienna Basin of Austria etc. Several other sandbox models are used for the quick propagations of faults. [3] presented a detailed analysis of the strike-slip fault by sand pack, which is applied by [1] [2] to analyze the Woodford El-Reno fault. Although [1] used wet clay model, the behavior of deformation by clay and sand exhibit certain similar characteristics. However, the selection of modeling materials could show differences. Dry sand does not show folding and localized faults, which is of significance as indicators for fractures. Thus to study the structure and its associated fractures of Woodford Shale, we applied the results from the wet clay rather than sandbox in analog modeling pull-apart basins.

Nonetheless, most of the analog models were applied to explain basins that could be mapped directly in field [4] [6]. As we know to date, few works were used to interpret basins in subsurface due to a lack of data and the difficulties to identify features of pull-apart basins.

Characterization of Woodford Shale basins is also challenged by its highly heterogeneous nature along with the lack of knowledge about these rocks. [1] [2] first applied the integrated method of the analog model and seismic analysis to study the El-Reno fault in Woodford Shale. It presented that seismic attributes help to illuminate field-scale geomorphologic features as well as build the basin-wide stratigraphic interpretations [1] [2]. In this research, we intend to extend this work further to explore the detailed subsurface structure. In previous work, we found that the El-Reno fault (ERF) is segmented into two master faults, which shows every feature relevant to a pull-apart basin at an early stage. Our goal in this paper is to identify potential sweet spots in this nascent pull-apart basin through careful analyses of seismic attributes based on current understanding of clay model proxies.

2. Regional Setting

The Woodford Shale was deposited in the palaeo-Oklahoma Basin, central USA during sea-level transgression (**Figure 1**) [8] [9] [10]. The Woodford Shale gently

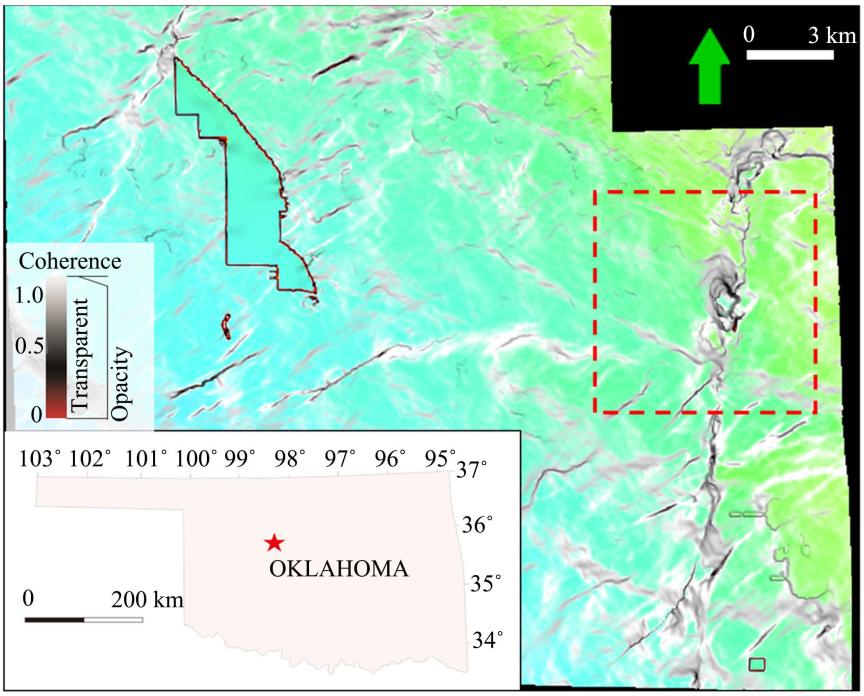

Figure 1. Two-way travel time (TWT) map of the top of the Woodford Shale, indicating its large-scale structure of the right-lateral strike-slip fault with a small-scale pull-apart basin (adapted from [2]). The time structure is co-rendered with the 3D determined coherence of a horizontal surface at this depth, gently dipping (<2˚) to the southwest. The dark lineaments (low coherence values or incoherence) reveal structural elements, including R faults of the strike-slip, the north-south fault zone, and the pull-apart basin within the red dashed box. Note transparent color is used for the high coherence area. Inset the location of the study area in the Anadarko Basin, Oklahoma (red star in Oklahoma).

dip (<2˚) towards southwest and the palaeo-shoreline is in the northeast [11]. Different petro-types are expected and Woodford Shale is proven within dry gas-condensate/oil maturity window in this study area, using a set of petrophysical properties tests at the University of Oklahoma. The porosity varies between 2% and 10%, bulk density varies between 2.2 g/cm^3 and 2.9 g/cm^3, and the Woodford Shale is a silica-dominated system; clay percentage varies between 20% and 70%, inversely proportional to the other dominated mineral, quartz; TOC ranges between 0 wt% and 14 wt%. In the group of samples with intermediate clay (8 wt% - 48 wt%) and quartz content (24 wt% - 58 wt%), TOC trends the same with increasing quartz, while in the other groups no relations were found. The mechanical property, e.g., elastic moduli, Young's modulus, varies inversely with TOC [11].

3. Materials and Methods

We used a 3D seismic survey in the Central Oklahoma to map an area of ~930 km^2 at the Woodford Shale level, at approximate depth of 4 km (data provided by CGG). **Figure 1** presents a time structure through the seismic coherence vo-

lume at the targeted Woodford Shale level. The major faults are indicated in gray-black, and the north-south striking fault on the eastern part is termed El-Reno fault (ERF). [1] [2] analyzed the 32 km long ERF as a typical strike-slip system with associated structures including Riedel shears, splay shears and P shears. We focused a distinct pull-apart basin along the ERF, which is ~1.6 km by 3.2 km in size and is bounded by secondary circular faults (**Figure 1**, within red dashed box). The pull-apart basin shows clear deep depressions of Woodford Shale. It connects the two major fault segments of ERF as principal displacement zone with rich structural information. We used seismic attributes and clay models to analysis the pull-apart basin and its associated fractures in this study.

4. Results

4.1. Pull-Apart Basin Model

The pull-apart basin could be simulated by conducting clay or sand models [3] [4] [5] [6]. We applied the results of wet clay models here for two reasons: 1) the clay model could present folds and detailed small faults; 2) the convenience of defining fault geometries and the possibility to study the mature structures with steep surfaces [6]. The experimental setup includes: 1) two metal plates, one sticking to a moving plate (0.001 cm/s) driven by motors and the other stable; 2) two soft clay cakes, one overlying on the metal plates as an analog of basement with a density of 1.85 g/cm^3 and a thickness of 2.5 cm, and the other overlying on the basement as an analog of sedimentary with a density of 1.6 g/cm^3 and a thickness of 2 cm. During the experiments, there is no shearing between the basement clay and metal plates. However, the basement clay deforms, releasing bends and offsets, which in turn controlling the deformation of the sedimentary layer. By such double-layer experiments, it overcomes the limitation to simulate basement offset by previous setups [5] [6] [12]. Photographs are taken during every stage of experiment. Laser scanning was involved to visualize the 3-D geometry and map the contours of the top surface of the sedimentary clay layer. The detailed method could refer to [6] from the University of Oklahoma.

The clay model is not a scale model of pull-apart basin but an analog to illustrate structures. A few distinct features are shown: 1) sidewall faults that are steep as boundary of the basin; 2) series of quasi-circular concave-upward faults (small Riedel shear faults) in the principle displacement zone to the descending basin center, with folds in between; 3) a few out-basin faults that are extended Riedel shear faults partitioning into the strike-slip fault. **Figure 2(b)** shows the late stage of clay experiment of pull-apart basin, with central part depressed downwards and faults striking ~45˚ at average. The depressed basin connected the two north-east segments of right-lateral strike-slip faults, with series of twisted Riedel faults indicated by black color. **Figure 2(c)** shows the contour map of the top of sedimentary layer. Contours in this figure are in intervals of 0.4 mm and every fifth contour is shown in black. The structural elevation with blue illustrates the basin center and yellow the high land. The denser contours in

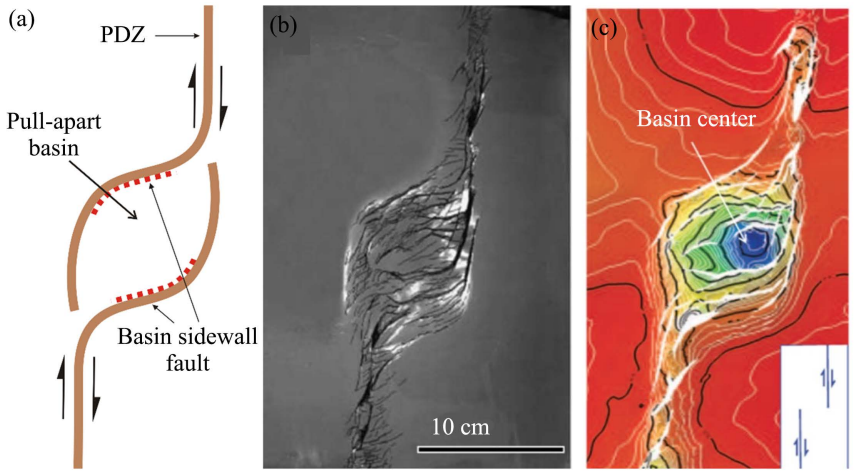

Figure 2. (a) Schematic model of a pull-apart basin and its photograph from clay experiment (b). (c) 3-D geometry of the top of the sedimentary clay surface. Contours in this figure are in intervals of 0.4 mm. Every fifth contour is shown in black. Blue color shows deepest point of the basin, while red means top. (Credit: Figure flipped and adapted from [6]).

southeast of the basin presents steeper depression. The total depressed depth in this experiment is estimated ~1.6 cm and the basin center is located toward the north segment of the controlling strike-slip fault. **Figure 2(c)** shows the out basin faults, sidewall faults, and inner connected twisted Riedel faults by digitizing the **Figure 2(b)**. Overall it is a typical pull-apart basin with asymmetric shape and the features complied with previous models [4] [6]. All these features were summarized as **Figure 2(a)**.

4.2. Attributes-Based Seismic Analysis

[2] studied the geological background of this study area, analyzed the major strike-slip fault vertically crossing the Woodford Shale, and indicated the shear deformation and secondary faults. It illustrated the development of surface folds, subsidence in the pull-apart depression, and sets of secondary faults, in particular the series of R and R' Riedel shears at angles of 18˚ and 70˚ with respect the main strike slip fault. It presented the complex evolution of the crooked strike-slip fault and the potential of a wide damage zone which is likely to host sub-seismic fractures and faults. We now integrate the attribute analysis to clay models aiming to reveal the detailed structure of the pull-apart basin. Three attributes (coherence, dip-azimuth, and curvature) calculated from 3D seismic survey are used to illuminate the fractures and faults.

The coherence is computed from seismic amplitudes on adjacent traces by a cross-correlation technique [13]. Coherence is used to identify lateral discontinuities with high values indicating discontinuities. We generated the 3D coherence volume, which is found best indicator of faults [14]. Co-rendering the coherence attribute with the time structure map of the top of the Woodford Shale reveals depositional pattern of the pull-apart basin. We used the structure pat-

tern in the wet-clay experiment (**Figure 2(a)** and **Figure 2(b)**) to interpret the pull-apart basin. The black color (**Figure 3(a)**) showed two quasi-circular sidewall faults, which depart from the main strike-slip fault at ~25˚. The east fault shows steeper fault surface (sidewall) than the west one. The extended out-basin fault also stand out as the splay faults if considered in the ERF fault system [1]. These features were further indicated by dip-azimuth map (**Figure 3(b)**). Dip-azimuth co-rendering on the time structure map shows the orientation of local dip and is used to assist the coherence analysis of the geological structures [1] [15]. In **Figure 3(b)**, it shows the west wall of the basin facing east and the other wall in the opposite. The area covered by pink color has been sheared and folded by NE-SW compression, which I interpret as fracture zones associated with anticlinal folds.

The correlation of a Gaussian curvature with outcrop fractures was first tested by [16]. In recent years, more efforts were put in this direction to compute multispectral volumes of curvature for subtle features and fractures [17]. Among all different curvature measures, the most-positive and most-negative curvature emerge as the most helpful tool to map anticlinal and synclinal flexures for their ability of multi-spectral analysis at different scales [15]. The curvature is found particularly effective indicator of folds which is highly relevant to high fracture intensity [1] [14] [18]. Inside the basin, curvature on time structure map (**Figure 4**) shows that a series of quasi-circular echelon normal faults step into the deepest parts of the basin with ~80 m of total subsidence. In addition, we found that curvature was the best indicator of the pull-apart structure. The most positive curvature (K1) zones clearly lineated folds that bound the basin, and the negative curvature area revealed the basin depression. It indicated the main features of this Woodward Shale basin are compatible with pull-apart features observed in ours and previous wet clay models.

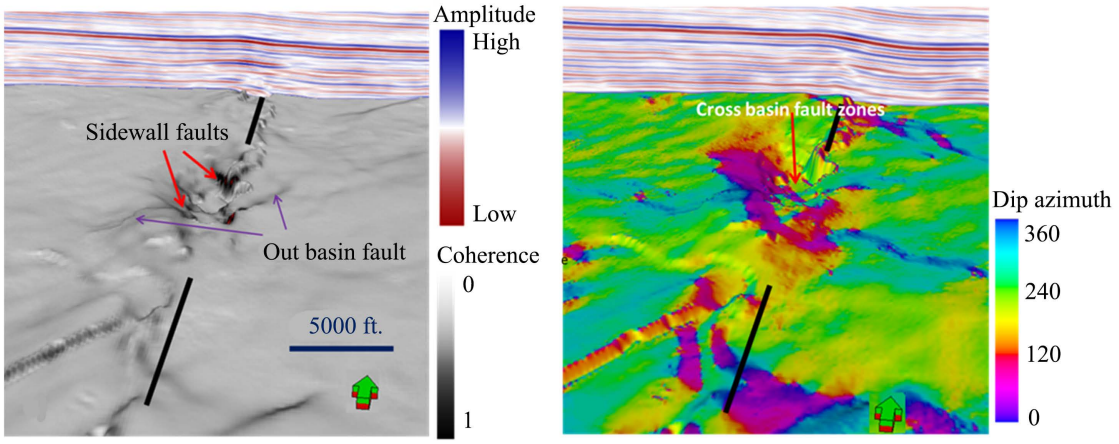

Figure 3. (a) A display of coherence co-rendered with seismic amplitude on the top of pull-apart basin within Woodford Shale. Black lines indicate two N-S master strike-slip faults. (b) Dip-azimuth map of the top of pull-apart basin within Woodford Shale. Bands of pink color within red dashed line boxes, revealing potential fracture zones with anticlinal compressed folds (Unit Conversion: 10 feet is about 3 meters).

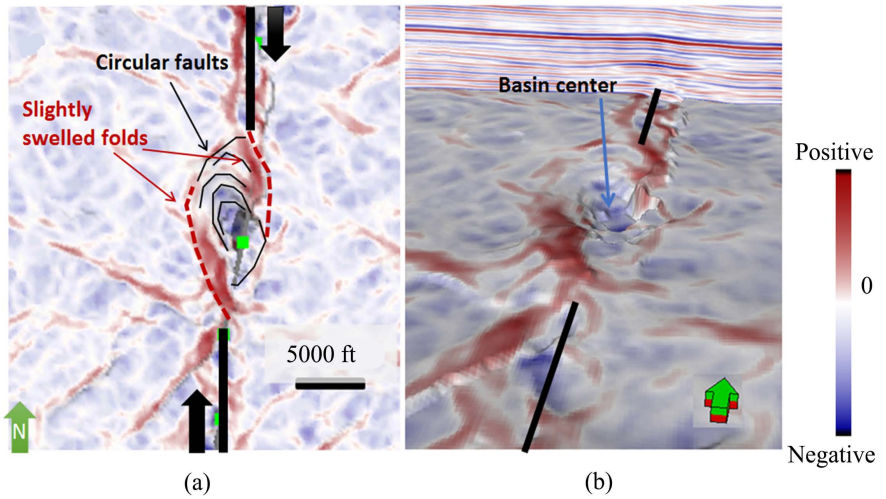

Figure 4. (a) Curvature on the top of pull-apart basin within Woodford Shale. Areas with strong curvature (brighter red and blue) correspond to strong flexures, folds, and densely fractures. (b) A 3D display of curvature on the top of a pull-apart basin within Woodford Shale. The connected line shows the N-S master strike-slip faults (Unit Conversion: 10 feet is about 3 meters).

In addition, we characterize the width of the pull-apart basin by measuring seismic attributes along transects across the basin (**Figure 5**). By computing the width of abnormal incoherence values of a series of transects in coherence map (**Figure 5(a)** and **Figure 5(b)**), it shows the basin width is about 1100 m in the northern part. Nonetheless, the most-positive curvature indicates the sidewall fault with anticlines in **Figure 5(c)**, which is commonly interpreted as sweet spots with high intensity of fractures [2].

5. Discussions

Pull-apart basins are zones of subsidence that resemble each other in a strike-slip region. It appeals to seismic interpreters to figure out the general structural patterns of pull-apart basins by using rheological concepts [4] [19]. For example, [4] demonstrated two rheological models for pull-apart basins, one is brittle-style, and the other one is ductile-style. The pull-apart basin usually develops between sub-parallel vertical segments [1], which is a typical feature of strike-slip faults [20]. The brittle-style sedimentary formations usually follow "Byerlee's rule" to fail and develop discrete and narrow faults. Such faults propagate toward each other, resulting in extensional and normal faulting of the basin (**Figure 6(a)**). The ductile-style maintains equal strength under stresses, and the faults creep into high maximum stresses zones away from each other, resulting in reverse faulting of the basin (**Figure 6(b)**). The rheological models are suggested in the interpretation process, which provides us insights to understand the structural pattern of the pull-apart basin. We confirm the brittle rheology for Woodford Shale that contains high quartz content ranging 24% - 58% in weight [11].

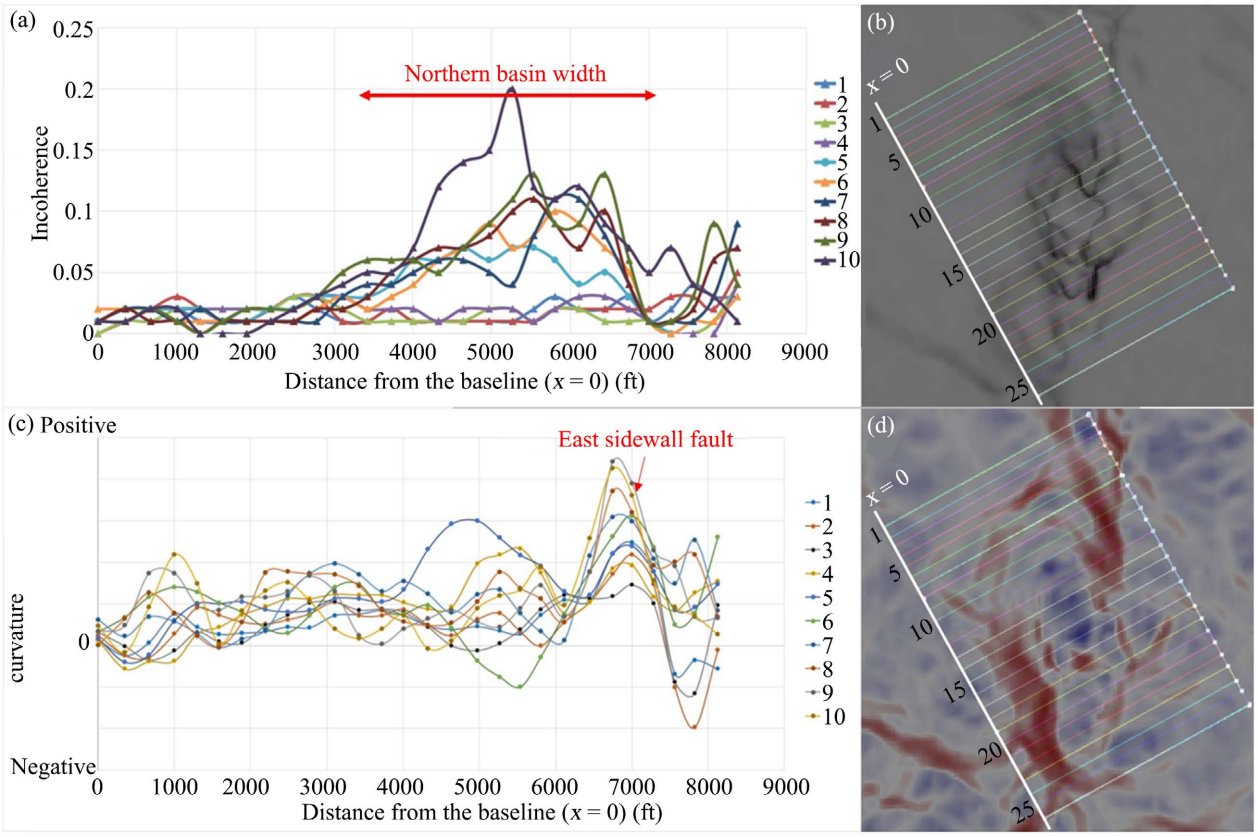

Figure 5. (a) Profiles of the coherence values across the pull-apart basin at the Woodford Shale level. Profile locations in (b). Note zones of incoherence values are interpreted as pull-apart basin region in the northern area. (c) Profiles of the curvature (K2) values across the pull-apart basin at the Woodford Shale level. Profile locations in (d). Note the most positive values are interpreted as east sidewall fault with anticline.

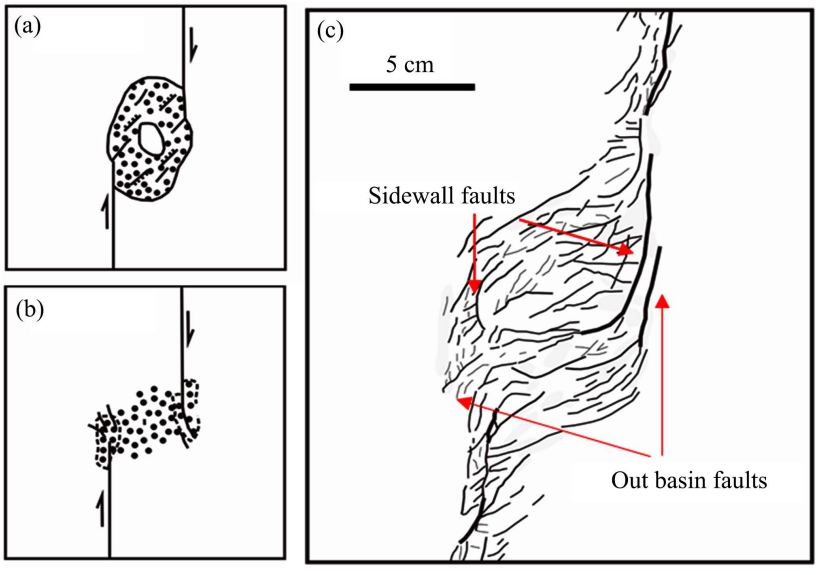

Figure 6. Predicted structures of a pull-apart basin in (a) brittle material and (b) ductile material (adapted from [4]). (c) Schematic faults observed on sedimentary clay surface in the clay experiments as an analog for the pull-apart basin (Figure flipped and adapted from [6]).

Another factor that may control the structural pattern of pull-apart basins is the relative positions of adjacent fault segments of a strike-slip [4] [5] [6]. In experimental modeling [6], if there is a bend fault connecting these two fault segments, the pull-apart basin will evolve from spindle-shaped, S-shaped, to rhomboidal-shaped with increasing bending angle; if there isn't a bend fault, the offset between the fault segments will allow distribution of strain over a larger area with more faults. The models demonstrate various possible structural shapes of a pull-apart basin in different configurations of strike-slip fault, which increases difficulties for interpreters with the discrepant understanding of fault evolutions. By selecting the right model could better indicate the proper structure features from seismic volumes; however, resemblance could serve as only an interpretation analog but not a sufficient criterion.

6. Conclusion

Current studies of the clay models illustrated the development of surface folds, subsidence in the pull-apart depression, and sets of secondary faults, in particular the pattern of basin-bounding faults and series of echelon faults stepping down into the bottom of basin. We applied such experimental observations and used three attributes (coherence, dip-azimuth, and curvature) to illuminate the features of pull-apart basin that connects two major El-Reno faults of the Woodford Shale, Oklahoma. We found that curvature was the best indicator of the pull-apart structure and the associated folds and faults. However, the analysis is still limited by its large resolution of hundreds of meters, which could be improved by integrating with various-scale data, e.g., logging image, and field observations in future research. We suggest that the subsurface structures of the pull-apart basin indicated by 3D seismic-attributes are likely to bear high intensity of fractures, which are potential sweet spots for horizontal drilling.

Acknowledgements

The authors would like to thank the reviewers for their thoughtful and detailed reviews for the manuscript, Chesapeake Energy and CGG-Veritas for providing licenses to their data. We also like to thank the sponsors of the Attribute Assisted Seismic Processing and Interpretation (AASPI), University of Oklahoma, and Z. Reches, N. Gupta, S. Chen, D. Pall, Z. Liao for their help. The authors declare no financial or other conflicts of interest.

Conflicts of Interest

The authors declare no conflicts of interest regarding the publication of this paper.

References

[1] Liao, Z., Liu, H., Jiang, Z., Marfurt, K.J. and Reches, Z. (2017) Fault Damage Zone at Subsurface: A Case Study Using 3D Seismic Attributes and a Clay Model Analog for

the Anadarko Basin, Oklahoma. *Interpretation*, **5**, 143-150. https://doi.org/10.1190/INT-2016-0033.1

[2] Liao, Z., Liu, H., Carpenter, B.M., Marfurt, K.J. and Reches, Z. (2019) Analysis of Fault Damage Zones Using Three-Dimensional Seismic Coherence in the Anadarko Basin, Oklahoma. *AAPG Bulletin*, **103**, 1771-1785. https://doi.org/10.1306/1219181413417207

[3] Naylor, M.A., Mandl, G. and Supesteijn, C. (1986) Fault Geometries in Basement-Induced Wrench Faulting under Different Initial Stress States. *Journal of Structural Geology*, **8**, 737-752. https://doi.org/10.1016/0191-8141(86)90022-2

[4] Reches, Z. (1987) Mechanical Aspects of Pull-Apart Basins and Push-up Swells with Applications to the Dead Sea Transform. *Tectonophysics*, **141**, 75-88. https://doi.org/10.1016/0040-1951(87)90175-2

[5] Dooley, T. and Mcclay, K. (1997) Analog Modeling of Pull-Apart Basins. *AAPG Bulletin*, **81**, 1804-1826.

[6] Mitra, S. and Paul, D. (2011) Structural Geometry and Evolution of Releasing and Restraining Bends: Insights from Laser-Scanned Experimental Models. *AAPG Bulletin*, **95**, 1147-1180. https://doi.org/10.1306/09271010060

[7] Crowell, J.C. (1974) Origin of Late Cenozoic Basins of Southern California. In: Dickinson, W.R., Ed., *Tectonics and Sedimentation*, Society of Economic Paleontologists and Mineralogists, Ponca City, Special Publications, No. 22, 190-204. https://doi.org/10.2110/pec.74.22.0190

[8] Lambert, M.W. (1993) Internal Stratigraphy and Organic Facies of the Devonian-Mississippian Chattanooga (Woodford) Shale in Oklahoma and Kansas. In: Katz, B.J. and Pratt, L.M., Eds., *Source Rocks in Admin Sequence Stratigraphic Framework*, AAPG Studies in Geology, No. 37, The American Association of Petroleum Geologists, Tulsa, 163-176. https://doi.org/10.1306/St37575C11

[9] Cardott, B. (2008) Overview of Woodford Gas-Shale Play of Oklahoma. *AAPG Annual Convention and Exhibition*, Midwest, 22 October 2008, 2-7.

[10] Paxton, S.T., Cruse, A.M. and Krystyniak, A.M. (2006) Detailed Fingerprints of Global Sea-Level Change Revealed in Upper Devonian—Lower Mississippian Woodford Shale of South-Central Oklahoma. *AAPG Annual Convention*, Houston, 9-12 April 2006, 9-14.

[11] Gupta, N., and Marfurt K.J., (2012) Multi-Scale Characterization of the Woodford Shale in West-Central Oklahoma: From Scanning Electron Microscope to 3D Seismic. Ph.D. Thesis, University of Oklahoma, Norman.

[12] Atmaoui, N., Kukowski, N., Stoeckhert, B. and Koenig, D. (2006) Initiation and Development of Pull-Apart Basins with Riedel Shear Mechanism: Insights from Scaled Clay Experiments. *International Journal of Earth Sciences*, **95**, 225-238. https://doi.org/10.1007/s00531-005-0030-1

[13] Bahorich, M.S., and Farmer, S.L. (1995) 3-D Seismic Discontinuity for Faults and Stratigraphic Features: The Coherence Cube. *The Leading Edge*, **14**, 1053-1058. https://doi.org/10.1190/1.1437077

[14] Staples, E. (2011) Subsurface and Experimental Analyses of Fractures and Curvature. M.S. Thesis, University of Oklahoma, Norman.

[15] Chopra, S. and Marfurt, K.J. (2007) Seismic Attributes for Prospect Identification and Reservoir Characterization. SEG Geophysical Developments Series No. 11, SEG Publisher, Houston. https://doi.org/10.1190/1.9781560801900

[16] Lisle, R.J. (1994) Detection of Zones of Abnormal Strains in Structures Using Gaus-

sian Curvature Analysis. *AAPG Bulletin*, **78**, 1811-1819. https://doi.org/10.1306/A25FF305-171B-11D7-8645000102C1865D

[17] Al-Dossary, S. and Marfurt, K.J. (2006) 3D Volumetric Multispectral Estimates of Reflector Curvature and Rotation. *Geophysics*, **71**, 41-51. https://doi.org/10.1190/1.2242449

[18] Sterns, D.W. (1978) Faulting and Forced Folding in the Rocky Mountains Foreland. In: Matthews III, V., Ed., *Laramide Folding Associated with Basement Block Faulting in the Western United States*, Geological Society of America Memoirs, No. 151, Boulder, 1-38. https://doi.org/10.1130/MEM151-p1

[19] Segall, P. and Pollard, D.D. (1980) Mechanics of Discontinuous Faults. *Journal of Geophysical Research*, **85**, 4337-4350. https://doi.org/10.1029/JB085iB08p04337

[20] Harding, T.P. (1985) Seismic Characteristics and Identification of Negative Flower Structures, Positive Flower Structures, and Positive Structural Inversion. *AAPG Bulletin*, **69**, 582-600. https://doi.org/10.1306/AD462538-16F7-11D7-8645000102C1865D